Biochimica et Biophysica Acta 1859 (2017) 1891–1899

Contents lists available at ScienceDirect

Biochimica et Biophysica Acta

journal homepage: www.elsevier.com/locate/bbamem

Crossregulation between the insertion of Hexadecylphosphocholine (miltefosine) into lipid membranes and their rheology and lateral structure

Yenisleidy de las Mercedes Zulueta Díaz, María Laura Fanani *

Centro de Investigaciones en Química Biológica de Córdoba (CIQUIBIC-CONICET), Departamento de Química Biológica, Facultad de Ciencias Químicas, Universidad Nacional de Córdoba, Haya de la Torre y Medina Allende, Ciudad Universitaria, X5000HUA Córdoba, Argentina

ARTICLE INFO

Article history:
Received 4 April 2017
Received in revised form 8 June 2017
Accepted 16 June 2017
Available online 20 June 2017

Keywords:
Amphiphilic drugs
Langmuir monolayers
Liposomes
Liquid-ordered domains
Stratum corneum mimicking membrane

ABSTRACT

Hexadecylphosphocholine (HePC, miltefosine) is an alkylphospholipid used clinically for the topical treatment of cancer and against leishmaniasis. The mechanism of action of HePC, not yet elucidated, involves its insertion into the plasma membrane, affecting lipid homeostasis. It has also been proposed that HePC directly affects lipid raft stability and function in cell membranes. The present work deals with two main questions in the understanding of the action of HePC: the bases for membrane selectivity and as a membrane perturbator agent. We explored the interaction of HePC with lipid monolayers and bilayer vesicles, combining monolayer penetration experiments, Brewster angle microscopy and differential scanning calorimetry. Several membrane compositions were tested to explore different rheological conditions, phase states and lateral structures. Additionally, the kinetics between the soluble and the membrane form of HePC was explored. Our results showed an increase in elasticity induced by HePC incorporation in all the membranes studied. Differential incorporation was found for membranes in different phase states, supporting a preferential partitioning and a higher dynamic kinetics of HePC incorporation into fluid membranes in comparison with condensed or liquid-ordered ones. This effect resulted in phase equilibrium displacement in phospholipids and membranes containing liquid-ordered domains. The presence of cholesterol or ergosterol induced a fast incorporation and slow desorption of HePC from sterol-containing monolayers, favoring a long residence period within the membrane. This contributes to a better understanding of the HePC regulation of membrane-mediated events and lipid homeostasis.

1. Introduction

Alkylphospholipids (APL) are stable analogues of lisophosphatidylcholine with antitumor activity [1]. Their mechanism of action involves insertion into the plasma membrane [1,2], affecting the biosynthesis of cholesterol (CHO) and phospholipids and the signaling pathways in which different lipid second messengers participate [3–5]. However, the detailed mode of action by which APLs exert their effect is still under debate. Some authors have reported their involvement in lipid raft stability, metabolism and apoptosis [2,5–7]. On the other hand, even though some APLs exhibit hemolytic effects, lysis does not appear to be their major mechanism of action [4,8]. This is supported by the fact that their median effective dose is in the same order as the critical micellar concentration (CMC) [4]. The monomeric form of the drug thus appears to play the main pharmacological role.

Hexadecylphosphocholine (HePC, miltefosine) is an APL used clinically for the topical treatment of skin metastases of cancer and cutaneous lymphoma as well as against the tropical disease, leishmaniasis [1,2,9]. Liquid-ordered (LO) nanodomains enriched in sterols and sphingolipids, named "lipid rafts" are proposed to exist in living cell membranes and regulate important cell functions. Besides fundamental differences, the existence of surface heterogeneity and liquid-liquid coexistence is expected to follow similar physico-chemical rules in natural membranes and model lipid membranes [10]. Several biophysical studies have aimed to clarify the action of HePC on sterol-containing lipid membranes; however, its effect is still controversial. HePC shows

Abbreviations: APL, alkylphospholipids; HePC, Hexadecylphosphocholine; POPC, 1-palmitoyl-2-oleoyl-*sn*-glycero-3-phosphocholine; DLPC, dilauroyl-*sn*-glycero-3-phosphocholine; DMPC, 1,2-dimyristoyl-*sn*-glycero-3-phosphocholine; DPPC, 1,2-dipalmitoyl-*sn*-glycero-3-phosphocholine; DSPC, 1,2-distearoyl-*sn*-glycero-3-phosphocholine; DMPS, 1,2-dimyristoyl-*sn*-glycero-3-phospho-L-serine; CER24, *N*-lignoceroyl-D-erythro-sphingosine; PSM, *N*-palmitoyl-D-erythro-sphingosylphosphorylcholine; ERG, ergosterol; CHO, cholesterol; CHO-S, cholesterol 3-sulfate sodium salt; SCM, stratum corneum mimicking membrane; LLC, liquid-liquid coexistence membranes; LA, lignoceric acid; LE, liquid-expanded phase; LC, liquid-condensed phase; LO, liquid-ordered phase; S, solid phase; π, surface pressure; Cs^{-1}, compressibility modulus; MMA, mean molecular area; BAM, Brewster angle microscopy; Lβ′, gel phase; Lα, liquid-crystalline phase; DSC, differential scanning calorimetry; Tm, phase transition temperature; ΔHc, phase transition enthalpy; ΔS, phase transition entropy; ΔT1/2, half width of the heat capacity peak; MLVs, multilamellar vesicles; LUVs, large unilamellar vesicles; LDS, dynamic light scattering.

* Corresponding author.
E-mail address: lfanani@fcq.unc.edu.ar (M.L. Fanani).

http://dx.doi.org/10.1016/j.bbamem.2017.06.008
0005-2736/

thermodynamic stabilization and film condensation when forming Langmuir films with CHO or ergosterol (ERG) [7,11–14], as has been found for other phospholipids [15,16]. This suggests an active role of HePC in stabilizing the LO phase, a hypothesis supported by dynamic simulations [17]. However, the incorporation of HePC into bilayer membranes shows no effect or induces destabilization of LO domains [7,18,19].

In this work, we explore the interaction of HePC with lipid monolayers as well as with bilayer vesicles. Various membrane compositions were tested, from pure phospholipid or sterol membranes to more complex lipid mixtures. The canonical ternary mixture that exhibits liquid-expanded (LE)/LO phase coexistence [20] was studied. Furthermore, since the pharmacological action of HePC involves skin penetration, a lipid mixture that mimics the lipid stratum corneum composition [21] was also included.

Previous studies by our group have shown that the incorporation of an amphiphilic drug into the membrane is closely regulated by its rheological properties [22]. When an amphiphilic molecule inserts into a membrane, an in-plane compression causes a lateral displacement of the other membrane components and, therefore, a lateral pressure opposes such incorporation. Thus, the ability of the membrane to respond to an isometric compression/expansion process may condition the insertion of a new molecule into the membrane. In the present work, we explore this regulation factor of the action of HePC.

Our work shows mutual modulation of the extent and kinetics of HePC insertion into the lipid membrane and the rheology, phase state and lateral structure of the target membranes. The equilibrium between the HePC present in different membrane structures was also explored. Our results provide evidence that casts light on the membrane selectivity reported for HePC as well as on its regulation of LO domains stability and membrane properties.

2. Materials and methods

2.1. Chemicals and reagents

Miltefosine or Hexadecylphosphocholine (HePC), 1-palmitoyl-2-oleoyl-*sn*-glycero-3-phosphocholine (POPC), 1,2-dilauroyl-*sn*-glycero-3-phosphocholine (DLPC), 1,2-dimyristoyl-*sn*-glycero-3-phosphocholine (DMPC), 1,2-dipalmitoyl-*sn*-glycero-3-phosphocholine (DPPC), 1,2-distearoyl-*sn*-glycero-3-phosphocholine (DSPC), 1,2-dimyristoyl-*sn*-glycero-3-phospho-L-serine (DMPS), *N*-lignoceroyl-D-erythro-sphingosine (CER24), *N*-palmitoyl-D-erythro-sphingosylphosphorylcholine (PSM), cholesterol (CHO) and ergosterol (ERG), were purchased from Avanti Polar Lipids, Inc. (Alabama, U.S.A.). Lignoceric acid (LA) and cholesterol-3-sulfate sodium salt (CHO-S) were provided by SIGMA-ALDRICH, Co (St. Louis, MO, U.S.A.). All other reagents were of analytical grade (99% pure) and used without further purification. The water was purified by a Milli-Q (Millipore,Billerica, MA) system to yield a product with a sensitivity of ~18.5 MΩ. The mixed monolayers used were: the anionic binary membrane containing DMPC:DMPS 70:30, membranes exhibiting liquid-liquid coexistence (LLC) composed of DLPC:PSM:CHO 33:33:34, and the stratum corneum mimicking membrane (SCM) composed of CER24/LA/CHO33:33:33 with the addition of 5% w/w CHO-S.

2.2. Monolayer experiments

Monomolecular lipid films were obtained as reported previously [22]. The Langmuir Isotherms, penetration and surface titration experiments were performed as described in Supporting Information.

Surface elasticity upon compression was assessed by means of the compressibility modulus (Cs^{-1}), which was calculated from the isotherm data as [23]:

$$Cs^{-1} = -MMA\left(\frac{\delta\pi}{\delta MMA}\right)_T \quad (S1)$$

where (π) stands for the surface pressure and (MMA) for the mean molecular area. The monolayers were observed while compressed, by Brewster Angle Microscopy (BAM) as described in Supporting Information.

2.3. Preparation and analysis of multilamellar vesicles

Lipid suspensions of DPPC or DPPC + HePC were prepared by hydration of a lipid film deposited on the wall of a glass test tube by solvent evaporation under an N_2 stream of a chloroform solution of lipids. This process leads predominantly to the formation of multilamellar vesicles (MLVs), as described before [24,25]. The lipids were hydrated with a buffer solution containing Tris-Base 10 mM, NaCl 120 mM and EDTA 0.1 mM (pH 7.4), applying vigorous mixing, and then subjected to ten freezing-thawing cycles (−195 °C and 50 °C, respectively). The final DPPC concentration was 2 mM, at which 0.2 mM (9 mol%) or 0.4 mM (16 mol%) of HePC were added. The effect of HePC on the size-distribution of the lipid suspension was studied by dynamic light scattering (DLS; Submicron Particle Sizer, NicompTM 380, Santa Barbara, California,USA) and analyzed in the nanometer range.

2.4. Differential scanning calorimetry (DSC) measurements

DPPC and DPPC + HePC lipid suspensions were also analyzed by DSC. The samples were subjected to a 15 min degasifying treatment before loading into a Microcal VP-DSC Scanning Calorimeter (Microcal, Northampton, MA, USA). The appropriate buffer was used in the reference cell. Thermograms were recorded over a temperature range from 20 to 60 °C, at a heating rate of 30 °C/h and analyzed with Microcal Origin 5.0 software (Microcal, Northampton, MA, USA) and Origin 8.0. Baselines were created and subtracted and then the plots were normalized according to the total lipid concentration. The deconvolution of multiple peaks curves was achieved by using PeakFit v4.12 software (SeaSolve Software Inc.).

The effects of HePC on DPPC vesicles were evaluated through different parameters: enthalpy and entropy changes (ΔH_C and ΔS) [26], transition temperature (T_m) and half-width of the transition peak ($\Delta T_{½}$).

2.5. Quantitative analysis of determination of soluble phosphorus

After the calorimetric runs, the lipid suspension was centrifuged at 13000*g* for 1 h at 4 °C in order to separate the MLVs from any unilamellar or micellar aggregate present in the sample [24]. Then, the supernatant samples were treated through the SEP-PAK C18 1 cm^3 VAC Cartridge 50 mg (Waters) and were eluted consecutively with ethanol and chloroform, obtaining a water, an ethanol and a chloroform fraction. Finally, each fraction was analyzed for phosphorus content using the method described by Bartlett et al. [27].

3. Results and discussion

3.1. Incorporation of HePC into monolayers with different rheology and phase states

In this work, we explored the interaction of HePC with lipid monolayers of different rheological characteristics combining penetration and superficial titration experiments. To study the incorporation of HePC into membranes, we used lipid monolayers on air/saline solution interfaces as model membranes. The monolayers composed of pure lipids were previously characterized as being in the phase states: POPC, liquid-expanded (LE); PSM and DPPC, liquid-condensed (LC); DSPC, solid (S) and CHO and ERG, liquid-ordered (LO) [22,28–33]. The last sterol was included since it is enriched in the plasma membrane of the *Leishmania* cells, an important HePC target. We also studied the binary mixtures of DMPC:DMPS (70:30), which contain a similar proportion of anionic lipids as most cell membranes and ternary mixtures

(DLPC:PSM:CHO, 33:33:34) that constitute the canonical membrane that exhibit liquid-liquid (LO-LE) coexistence (named liquid-liquid coexistence membranes or LLC) [20]. Furthermore, a quaternary mixture that mimics the uppermost layer of the skin, the stratum corneum (SCM) (CER24/LA/CHO, 33:33:33 with addition of 5% w/w CHO-S) [21,22], was studied, since this lipid-based structure represents an important barrier for HePC action in cutaneous Leishmaniasis.

The assignation of a phase state to a lipid monolayer is based on its elastic response to dilatational stress (i.e., the compressibility modulus, Cs^{-1}, see Fig. 1A) and the shear viscosity properties by comparing the bidimensional diffusion of latex beads in the monolayer plane [22]. A low Cs^{-1} value indicates that the lipid film is easily compressible, a typical behavior of LE monolayers [23]. LO, LC, and S monolayers show higher Cs^{-1} (see Fig. 1A) but with different diffusional properties: the components of LO membranes have as high a lateral diffusion dynamic as in an LE phase [32], while lipids in the LC phase diffuse more slowly and the domains show rounded borders. In contrast, lipids in the S phase have a severely restricted lateral dynamic and the S domains show irregular borders [22].

When HePC is added to a saline solution it aggregates into micellar structures above the CMC. Early studies reported values of CMC of 2–2.5 μM for HePC in 150 mM NaCl solution [13]. However, a recent detailed study shows that HePC aggregates in a salt dependent manner with a CMC of 40 ± 20 μM at the same salt concentration used in our studies, depending on the method employed [34]. On the other hand, a median effective dose of 2.5 to 6.5 μM was reported for HePC [4]. For our monolayer studies we choose a final concentration of 13 μM, which falls into the CMC range reported but above HePC median effective dose concentration. HePC spontaneously adsorbs into the air/water interface inducing a fall in its surface tension of (or an increase in surface pressure) of 30–34 mN/m at equilibrium [13,34]. However, when a lipid monolayer is previously placed at the interface, HePC can penetrate the membrane up to higher surface pressures (π) (Fig. 1B).

Fig. 1A shows that HePC can penetrate lipid films that initially are at 30 mN/m, a π close to that estimated for lipid bilayers [35]. HePC alters the film properties when incorporated into the membrane, as is evident by comparison of the Cs^{-1} parameter of the films before and after the penetration process reached equilibrium. Our results show that the drug decreased Cs^{-1} values, indicating that HePC has the ability to convert the films into more compressible monolayers in all cases. This decrease was approximately of 50% in all membranes studied, with the exception of the DMPC:DMPS and SCM films. Those anionic monolayers exhibited a greater resistance to compression (Cs^{-1} decrease only 30–35%), probably due to in-plane electrostatic repulsion given by a high density of negative charges. As will be discussed below, this effect also explains a scarcer insertion of HePC into negatively charged membranes. This decrease of Cs^{-1} induced by HePC agrees with previous reports supporting an increase of cell membrane fluidity after HePC incorporation [18,34,36].

From these experiments, we determined values of π achieved after the insertion of HePC into the monolayers. We found that the drug is able to increase the π in 10–23 mN/m of lipid monolayers initially at 30 mN/m. The higher effect was obtained for membranes with LC character (PSM and SCM), whose increase in π reaches double that observed in the rest of the membranes. Our results show that the increase in π roughly follows the order LC > LO > LE > S (Fig. 1B). The π increase of ~14 mN/m for HePC insertion into POPC and ERG monolayers agrees with previously reported values of 12 mN/m [13], and thus from this data we may infer that a similar incorporation extent occurs for both monolayers (which is not the case, as discussed below).

A similar study was performed previously by our laboratory for a different drug family but with comparable amphiphilic character. We found that the increase in π does not directly correlate with a higher incorporation of the drug [22]. Thus, the observable π increase is a consequence of at least two factors, (i) the amount of drug incorporated into the lipid film and (ii) the sensitivity of the lipid film to the drug incorporation, which is the mechanical properties of the hosting film. Therefore, we further tested the HePC uptake capacity of lipid monolayers at 30 mN/m by means of surface titration experiments.

Fig. 1B shows the HePC molar fraction necessary to achieve 50% saturation π ($\times_{50}$) by the surface titration test. Our results clearly show that a large increase in π is not necessarily indicative of greater incorporation of the drug into the monolayers. The membranes with LE character showed a smaller π increase than LC membranes, but they reached the greater incorporation reflected in high values of $\times_{50}$ (0.18–0.28). The membrane with S phase state showed the smallest increase in π and a poor insertion of HePC. On the other hand, the membranes

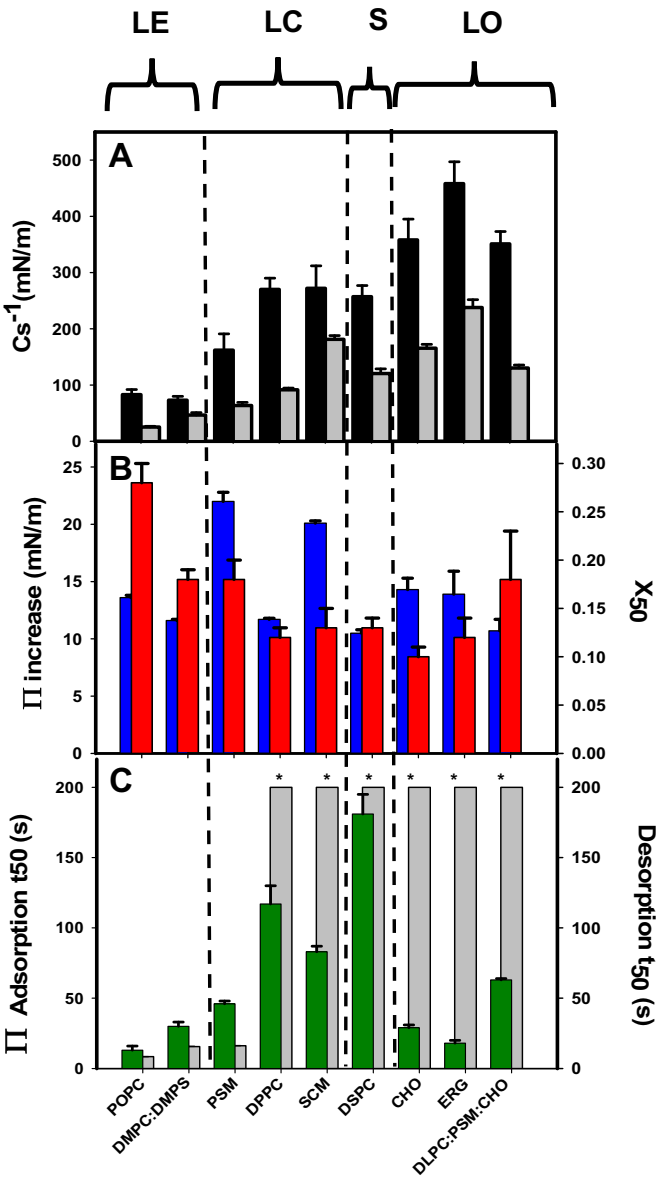

Fig. 1. Insertions of HePC into monolayers with different rheological character at 30 mN/m. A) Comparison of the mean values of compressibility modulus (Cs^{-1}) of monolayers in the absence (black bars) and after equilibration with HePC in the subphase (gray bars). B) π increase after the insertion of HePC into the acceptor monolayers and equilibration (blue bars). The plot also shows the molar fraction of HePC necessary to achieve 50% saturation π ($\times_{50}$) by the surface titration test. C) Kinetic parameters of the insertion of HePC into the acceptor monolayers: adsorption and desorption kinetics were calculated by fitting a hyperbolic function of the time course of HePC penetration and the relaxation after surface saturation, respectively. t_{50} represents the time for reaching 50% of the adsorption or desorption process. The asterisks indicate values of t_{50} > 1200 s. The letters refer to the phase state of the films: liquid-expanded (LE), liquid-condensed (LC), solid (S) and liquid-ordered (LO). Error bars in all graphics correspond to the Standard Error of the Mean (SEM) of triplicate experiments.

containing sterols showed an intermediate behavior with little incorporation of the drug.

A close inspection of Fig. 1A and B highlights an inverse correlation between drug incorporation ($\times_{50}$) and the Cs^{-1} values of the lipid films (before HePC treatment). This effect reflects the importance of the compressibility properties of the membrane in the insertion process, as has been found before for other amphiphilic drugs [22]. Also, the presence of a negatively charged membrane appears as an inhibitor factor for HePC incorporation. This can be explained as the result of an electrostatic repulsion that opposes lateral compression of the anionic molecules by the incoming drug molecule. We also calculated the mole fraction of the HePC at equilibrium pressure, assuming ideal mixing behavior for the drug/lipid system as describe in ref. [22] and obtained results with a similar trend to those obtained for $\times_{50}$ for the different monolayers (data not shown).

Several studies have explored the surface interaction between HePC and sterols in comparison with the HePC-phospholipid interaction by using Langmuir films [11–14]. Those studies did not explore the insertion of HePC from the aqueous subphase but forced the system to coexist in the air/water interface during the experimental time. From those works, a favorable interaction of HePC and sterols was observed, based on the finding of a molecular area condensation effect and a favorable excess free energy of mixing. These strong attractive lateral interactions between CHO and HePC were understood as the formation of a surface complex, as a consequence of a complementary molecular geometry of the interacting molecules: HePC possesses a conical shape, which in combination with CHO, an inverted cone-shaped molecule, ensures favorable packing of the mixed film [14].

We did not find that this favorable HePC-sterol lateral interaction influenced the incorporation of the HePC monomer (from the aqueous subphase) into sterol-containing monolayers, in equilibrium conditions. Therefore, we further explored whether the presence of sterols (and in general the rheological properties of the membrane) alters the dynamics of HePC insertion into the membranes. The kinetic parameters (t_{50}) shown in Fig. 1C were calculated from the time curves for HePC penetration (into lipid films) and desorption (from HePC saturated films).

The more fluid monolayers showed faster adsorption/desorption kinetics than condensed membranes (Fig. 1C). On the other hand, monolayers containing sterols allowed a relatively scarce but rapid insertion and a very slow desorption (compare Fig. 1B and C). The slow desorption found may be related to the strong lateral interactions between the CHO or ERG with HePC when coexisting in the membrane plane [11–14]. The order of magnitude difference of almost two in the adsorption/desorption kinetic parameters implies that the HePC molecules incorporated into a sterol-rich membranes will remain kinetically trapped in far-from-equilibrium conditions. Since all living systems occur in such conditions, an effective higher incorporation of HePC in cell membranes with a high content of sterols may be of importance in its pharmacological effect. Matching our results a slow desorption of a close related drug, edelfosine, from sterol-enriched compared with phospholipid-enriched liposomes has been previously reported and this capacity has been related with the haemolytic activity of the binary preparation [37]. This was interpreted by the authors as a consequence of a complementary molecular shape that favors plane bilayers stability.

3.2. Preferential partitioning of HePC into heterogeneous membranes by Brewster angle microscopy

The above results indicate that HePC has a higher insertion in membranes with a LE character compared to sterol-containing membranes. To further test this hypothesis, we extended this study to the effect of HePC on heterogeneous membranes. The preferential partitioning of the drug was evaluated on DPPC membranes with LE/LC phase coexistence [38,39] and LLC membranes, which show LE/LO phase coexistence [20], by Brewster angle microscopy (BAM). This technique enables the microstructure of the films to be assessed. Since the gray level of BAM images depends on both the refraction index of the film and the monolayer thickness [40], the LE phase appears as darker regions in the image in comparison with the LC or LO domains, which show a thicker and/or more compact nature.

Monolayers of pure DPPC exhibited LE-LC phase transition with phase coexistence in the π range of (5–17) ± 1 mN/m (Fig. 2A, B), as has been previously reported [38]. LC domains nucleate and grow above 5 mN/m, forming curved-branch domains. These typical shapes respond to a chiral crystalline structure of DPPC molecules in the LC phase [39,41]. The crystalline structure is evidenced by BAM imaging, which reveals optical anisotropy due to a tilted arrangement of the ordered acyl chains of DPPC [42]. This effect is observed as a continuous variation of the brightness level as one follows the long axis of the branches (Fig. 2A). Above 17 mN/m, a near-uniform phase of LC character was observed, which conserves the anisotropic organization (Fig. 2A). On the other hand, pure HePC Langmuir monolayers have been reported to form LE films at all π until the collapse at ~35 mN/m [13,43], as shown in Fig. 2B.

DPPC films containing 20 mol% of HePC showed an increase in the span of the phase coexistence region, shifted to higher π (15 to 35 ± 1 mN/m), as can be seen from the BAM images and the compression isotherm (Fig. B, C). Concomitantly, the LC domains showed rounded shapes but still keeping the optical anisotropy effect, as shown in Fig. 2C. This finding indicates the maintenance of a near-pure DPPC crystalline structure. A quantitative analysis of BAM images, such as those shown in Fig. 2A and C, was performed at 15 mN/m, and revealed that the LE phase increased from 4 ± 1 to 96 ± 1% as a consequence of the presence of HePC (20 mol%). This evidences a thermodynamic stabilization of the LE over the LC phase, which implies that HePC mixes preferentially into the LE and scarcely into the coexisting LC phase, as has been suggested from the surface titration results shown in Fig. 1B. Fig. 2B also shows that the compression isotherm of the mixed Langmuir monolayer has intermediate characteristics in relation to the pure component isotherms. However, at high π, the behavior closely resembles that of pure DPPC, showing similar Cs^{-1} values (not shown) and collapse π, probably due to partial expulsion of the drug from the monolayer.

The LLC mixed film shows the coexistence of liquid phases, as can be observed by the presence of rounded light gray domains (LO phase) surrounded by a darker gray area (LE phase) in BAM images (Fig. 3A) at π below the merging pressure (20 ± 2 mN/m). The corresponding compression isotherm shows a scarcely compressible film at high π (Fig. 3B), in accordance with an LO character [20].

In the presence of 20 mol% of HePC, it was observed that the merging π shifted to higher values (34 ± 1 mN/m). Furthermore, HePC induced the formation of nanodomains from very low π that coarsen into larger domains near the merging π (Fig. 3C). This suggests that the presence of the drug favors domain nucleation, probably altering the line tension between the coexisting phases [10,44]. The corresponding compression isotherms are shown in Fig. 3B. The LLC mixture with 20 mol% of HePC showed an intermediate behavior compared to the control isotherms.

A quantitative analysis of the images in Fig. 3A and C at 15 mN/m reveals that the percentage of the area occupied by the LE phase increased from 11 ± 1 to 49 ± 1% in the presence of the drug. In addition, we calculated the levels of reflectivity of each coexisting phase from the image gray level data [40] and found that the LE phase decreased ~28% its reflectivity in the presence of the drug, while the LO phase remained constant. These results support the hypothesis that the HePC preferentially partitions into the LE phase when in coexistence with an LO phase, in agreement with our surface titration results. This correlates with previous studies made in lipid vesicles that report an LO/Lα partition coefficient of ~0.5 for a fluorescence analogue of HePC [18].

3.3. Interaction of HePC with phospholipid bilayers

In the previous section, we showed that HePC is able to shift lipid phase transitions in lipid monolayers by partitioning preferentially

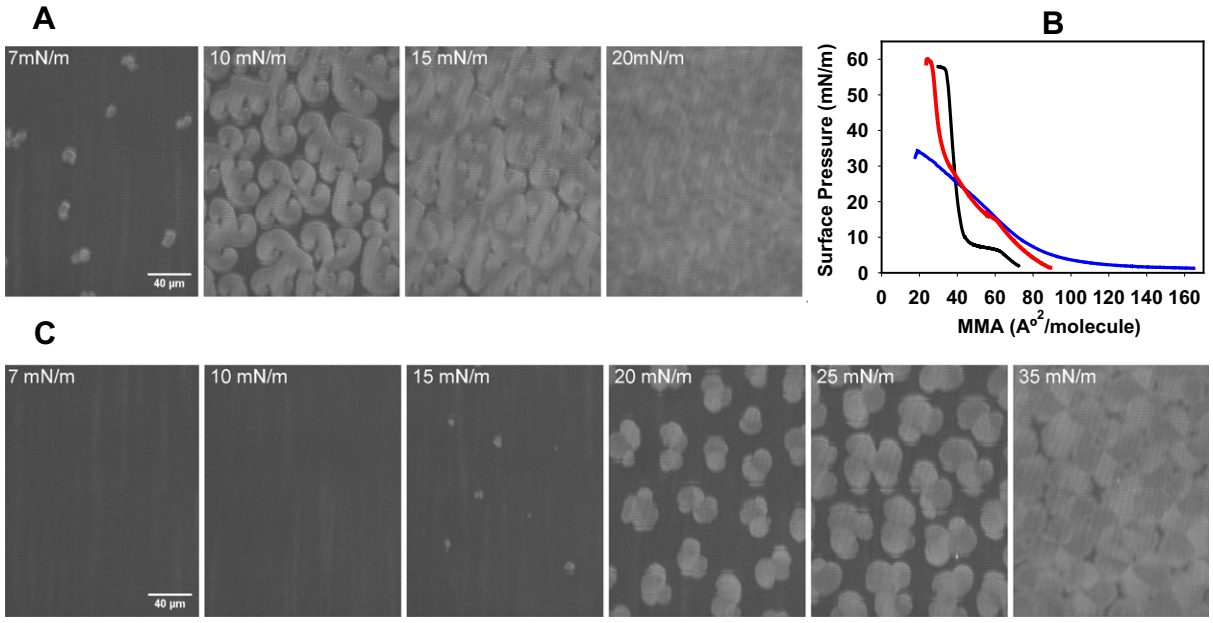

Fig. 2. Visualization by Brewster Angle Microscopy of DPPC under isothermal compression in the absence (A) and presence (C) of 20 mol% of HePC. The bright areas correspond to the LC phase in equilibrium with the LE phase (darker areas). The images are representative of two independent experiments. T: 22 ± 1 °C. B) Compression isotherms of Langmuir monolayers composed of pure HePC (blue), pure DPPC (black) and DPPC + 20 mol% of HePC (red). The curves are representative experiments, varying <2 mN/m of their corresponding replicates.

into the more expanded phase. We further studied whether the same effect occurs in a model bilayer membrane. Differential scanning calorimetry (DSC) was used to investigate the thermotropic properties of DPPC and DPPC-HePC acqueous suspensions. Fig. 4 shows the DSC endothermic profile for pure DPPC and mixtures of DPPC + 9 and 16 mol% of HePC, which correspond to a final HePC concentration of 0.2 and 0.4 mM. Those values are far above the CMC measured for HePC in the absence of lipid membranes [34]. However, the organization of HePC in micellar structures might be strongly influenced by the presence of DPPC MLVs, as demonstrated below.

DPPC suspensions show two endothermic peaks corresponding to pre- (gel to Lβ′) and main (Lβ′ to Lα) transitions, in agreement with the literature [45,46] (see Fig. 4A and Table 1). Pure HePC aqueous suspensions did not give any peak in the thermograms (not shown). The addition of HePC to DPPC suspensions caused the elimination of the pretransition, as has been observed for other phospholipid-drug

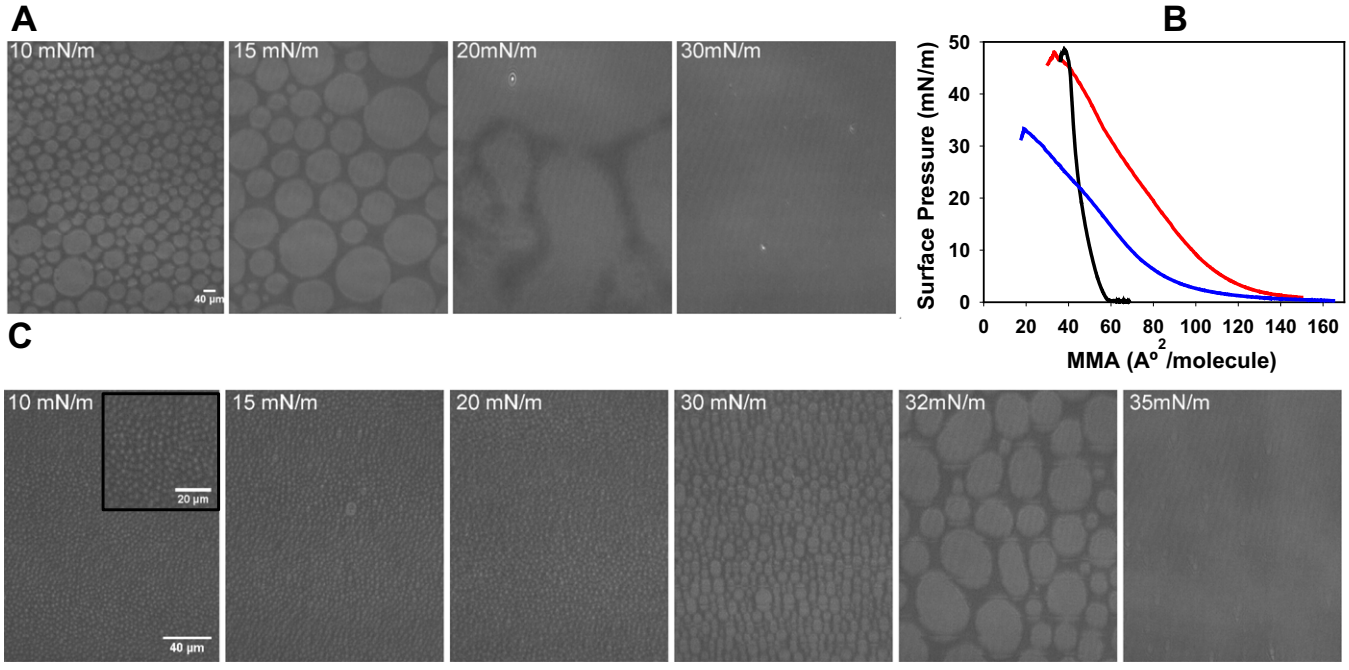

Fig. 3. Visualization by Brewster Angle Microscopy of LLC mixtures containing DLPC:PSM:CHO (1:1:1) under isothermal compression in the absence (A) and presence (C) of 20 mol% of HePC. The bright areas correspond to the LO phase in equilibrium with the LE phase (darker areas). The images are representative of two independent experiments. Inset shows the BAM image of the mixed monolayer at 10 mN/m at a larger magnification. T: 22 ± 1 °C. B) Compression isotherm of Langmuir monolayers composed of pure HePC (blue); DLPC:PSM:CHO (1:1:1), (black) and DLPC:SM:CHO (1:1:1) + 20 mol% of HePC (red). The curves are representative experiments, varying <2 mN/m from their corresponding replicates.

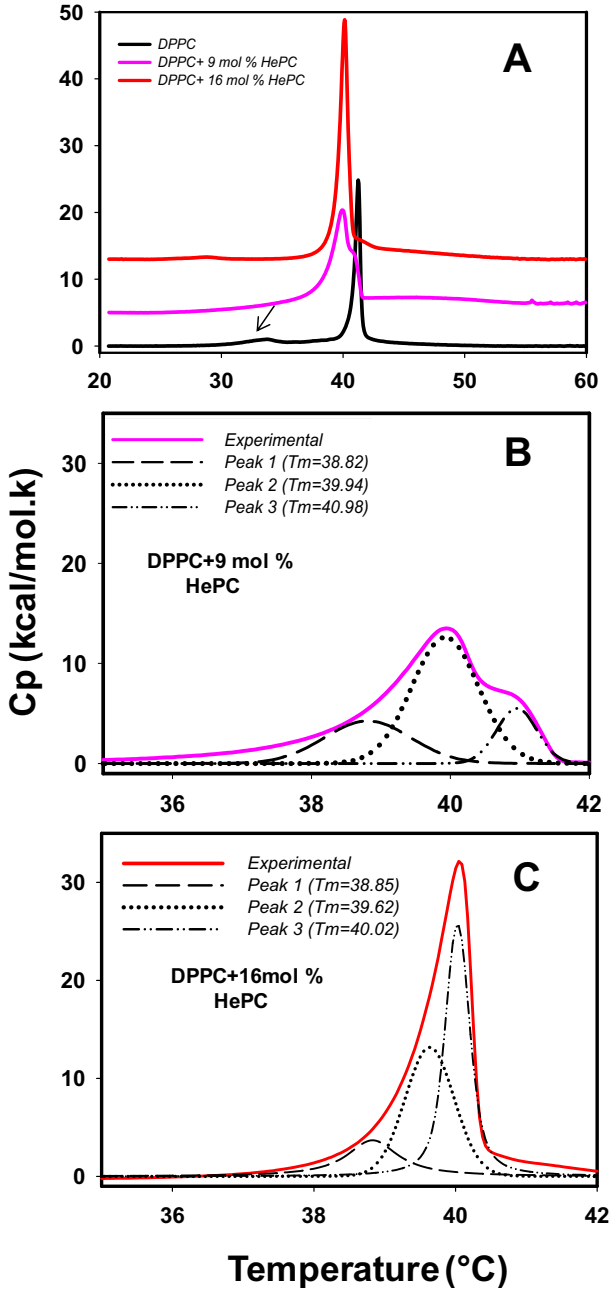

Fig. 4. Representative DSC heating thermograms of DPPC-HePC aqueous suspensions. A) Thermograms of pure DPPC (black) and mixtures of DPPC + 9 (pink) and 16 mol% (red) of HePC. Deconvolution peaks and the corresponding thermograms of samples containing DPPC + 9 (B) or16 (C) mol% of HePC. The heating rate was 30 °C/h. The arrow in (A) indicates the DPPC pretransition.

systems [45]. We also observed a shift of the main transition to lower temperatures, quantified as a lowering by 1.3 °C of Tm. Additionally, the broadening of the calorimetric peak, evidenced by an increase in the half width of the peak ($\Delta T_{1/2}$) [26], indicated loss of cooperativity in the process (Fig. 4A and Table 1).

A deconvolution analysis of the main transition peak of DPPC-HePC system was performed by the application of a non-two state transition model. Fig. 4B shows that the presence of 9 mol% of HePC induces the main transition peak to appear as composed of three components. The third peak appeared around 41 °C and would correspond to that of near-pure DPPC. When 16 mol% HePC was present in the sample, three peaks were also calculated to contribute to the thermogram (Fig. 4C). The different peaks contribute in different proportions to the complete calorimetric transition. It can be observed that the peak with the largest contribution shifts to lower temperatures as the HePC concentration increases (Fig. 4). Furthermore, the lack of a peak near 41 °C in the 16 mol% of HePC sample suggests saturation of the lipid membrane in the 9–16 mol% concentration range.

Table 1 shows a strong increase in the transition enthalpy (ΔHc) upon the addition of HePC. This increase in ΔHc evidences a more favorable van der Waals interaction between the long-chained DPPC and the hydrophobic part of HePC in the gel phase bilayer core [47]. A greater than two-fold increase was also obtained for the transition entropy (ΔS) in the presence of HePC, which may be explained as a better mixing of HePC into the fluid phase. This, along with a decrease in T_m, reflects a thermodynamically more favorable transition to the Lα phase in the presence of HePC than for pure DPPC, and supports a preferential partitioning of HePC into fluid phases, as observed in the previous section.

Taking into account that HePC shows a relatively high CMC (in the micromolar range) [13,34] compared to phospholipids, which are typically in the nanomolar range [47], we explored the partition between the water-soluble and membrane-bound form of the drug. We subjected the DPPC-HePC water suspension used for DSC analysis to centrifugation and physical separation of the soluble and membrane fractions. The soluble fraction was further processed through reversed phase (C18) chromatography and three fractions were obtained: aqueous, ethanol and chloroform fractions. The quantitative analysis of phosphorus content in each chromatographic fraction is shown in Table 2.

Pure DPPC suspension showed <3% recovery in the soluble fractions, indicating that 97% of the phospholipids precipitated during the centrifugation process, as reported before [24]. We also analyzed HePC aqueous suspension, from which about 88% of the total drug was recovered in the soluble fractions (Table 2). It is worth noting that, from the recovered HePC molecules, 95% eluted in the ethanol fraction. Therefore, when analyzing mixed DPPC-HePC samples, we can fairly assume that the phosphorus contributed from HePC molecules mainly elutes in the ethanol fraction, while the phosphorus coming from the more hydrophobic DPPC molecules was recovered mainly in the chloroform fraction.

In samples containing 9 mol% of HePC, only 16% of the total drug was recovered in the soluble fractions, indicating that the rest was present in the membrane fraction. This, in turn, represents an enrichment of ~8 mol% of the drug in the DPPC membranes, organized as MLVs [25]. For samples containing 16 mol% of HePC, a larger amount of drug was recovered in the soluble fraction (Table 2). In this case, the membrane fraction retained an amount of drug that represents only 10 mol% of the membrane components.

These results suggest that, at the highest drug concentration explored, the system was close to drug saturation. This finding roughly

Table 1
Thermodynamic parameters from the analysis of DSC data of DPPC in the absence or presence of 9 or 16 mol% of HePC.

Sample	Pre-transition		Main transition			
	Tm (°C)	ΔHc (kcal/mol)	Tm (°C)	$\Delta T_{1/2}$ (°C)	ΔHc (kcal/mol)	ΔS (kcal/mol.K)
DPPC	33.6 ± 0.1	2.1 ± 0.2	41.3 ± 0.1	0.46 ± 0.03	8.6 ± 0.1	0.027 ± 0.001
DPPC + 9 mol% HePC			40.1 ± 0.1	1.79 ± 0.06	20.7 ± 0.8	0.066 ± 0.002
DPPC + 16 mol% HePC			40.03 ± 0.05	0.65 ± 0.03	17 ± 2	0.06 ± 0.01

Table 2
Quantification of phospholipids in reversed phase chromatography elution fractions.

Samples	% of recovery of the ethanol fraction[a]	% of recovery of chloroform fraction[a]	% of recovery of the aqueous fraction[a]
DPPC	0.5 ± 0.1	1.7 ± 0.1	0.3 ± 0.1
HePC	84 ± 2	3 ± 1	0.6 ± 0.3
DPPC + HePC 9 mol%	16 ± 2	3.3 ± 0.2	1.8 ± 0.7
DPPC + HePC 16 mol%	46.6 ± 0.7	9 ± 2	3 ± 1

[a] The error corresponds to the SEM of duplicated samples.

agrees with a half-saturation ($\times_{50}$) of 12 mol% in DPPC monolayers, as obtained by surface titration experiments (Fig. 1B).

Table 2 also shows a considerable increase in the chloroform fraction for samples containing 16 mol% of HePC, suggesting that ~9 mol% of the DPPC molecules were present in smaller structures that did not precipitate under centrifugation treatment. We further analyzed the effect of HePC on the size particle distribution of the lipid suspensions in the nanometric range by dynamic light scattering (DLS).

DPPC suspension showed the presence of large particles (>800 nm, Fig. 5), corresponding to MLVs, as expected. Micrometric size structures are probably present but not analyzed in the present work. On the other hand, pure HePC samples presented a population of small particles (10–20 nm), which correspond to micelles and a different population in the 50–100 nm range that may include cylindrical micelles or small vesicles. In the presence of 9 mol% of HePC, the smallest size population becomes less important and a new population appears at ~300 nm. A further increase in HePC content resulted in a single population in the nanometer range centered at 100 nm. This, along with an increased amount of phosphorus present in the chloroform fraction for this sample, indicated that the drug induces restructuring of part of the DPPC molecules into intermediate sized particles, which may correspond to unilamellar vesicles, whist HePC micelles were no longer present. Our results correlates with reports where a fluorescent analogue of HePC at low concentration induces disorder in DPPC liposomes while at concentration above 10 mol% promoters large changes in the bilayers including loss of integrity and the formation of structures containing lipids, drug and the fluorescent probe [34].

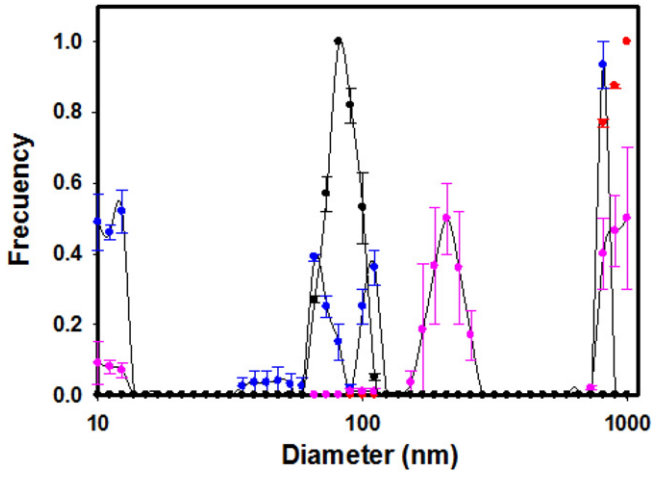

Fig. 5. Analysis of the size distribution by DLS of DPPC and DPPC-HePC suspensions in the nanometer range. The samples were hydrated suspension of HePC 0.4 mM (blue), DPPC 2 mM (red), and DPPC containing 9 mol% (pink) and 16 mol% of HePC (black). The data corresponds to the average value from two independent experiments, the bars corresponding to the SEM.

4. Conclusions

The present work deals with two important questions, HePC membrane selectivity and its action as a membrane perturbator agent. Several APLs are known to have selectivity for cancer cells over normal cells, even showing different sensitivities among various tumor cells [1,2]. Furthermore, HePC has different selectivity against different *Leishmania* species [7,48,49]. Our monolayer study strongly suggests that these different sensitivities may be related to differences in the rheological properties of the cell membranes. Expanded membranes, such as those composed of unsaturated phospholipids, had a larger uptake of HePC than condensed membranes and also than sterol-containing membranes. This matches reports of an enhanced accumulation of saturated phospholipids and CHO in HePC-resistant *Leishmania* Promastigotes [48].

On the other hand, those LE membranes also showed a faster adsorption/desorption dynamic, while condensed monolayers show a slower dynamic. Additionally, sterol-containing membranes show an unexpected combination of a rapid membrane adsorption and an almost irreversible uptake (in the experimental time scale). In this regard, LO membranes may favor a longer residence time for HePC molecules under far-from equilibrium conditions, such as those in living cells.

Cell membranes are conceived to be mostly in the liquid-crystalline (Lα) phase [47], a state closely related to the LE phase in monolayers. However, an enrichment in CHO or ERG might favor the occurrence of lipid rafts: nano-size LO domains proposed to be involved in a large number of cellular functions [10,50]. A high content of CHO or ERG in plasma membranes can act as a drug attractor center in non-equilibrium processes. This opens up a different dimension in the understanding of the effect of sterol content on the mode of action of HePC.

There is solid data that a favorable HePC-sterol interaction is seen when laterally coexisting in a membrane arrangement [7,11–14]. Even though this appears to contradict the low uptake data found in the present work, this effect can explain the finding of a very slow desorption of HePC from a sterol-containing membrane. This stabilization effect may also be responsible for the inhibition of CHO transport from the plasma membrane to the endoplasmic reticulum by HePC found in cell cultures [5]. On the other hand, the insertion of a monomeric HePC molecule from aqueous media into the sterol-enriched membrane (adsorption process) appears as a fast event but with a relatively impaired extent. This process implies the lateral compression/displacement of the other membrane molecules to place a new HePC one. Thus, the rheological properties of the membrane became relevant [22].

Previous studies with a different amphiphilic drug family evidenced an inverse correlation between the Cs^{-1} of lipid films and their capacity of drug incorporation [22]. This effect may be understood since, in films with high Cs^{-1}, a small lateral compression induced by the incoming drug molecule is responded to with a high increase in lateral surface pressure. This, in turns acts as a counteracting force against drug incorporation. A clear inverse correlation of Cs^{-1} vs. drug incorporation is also found in the present work.

CHO–enriched films show high Cs^{-1} without resigning the fluidity of the membrane [22]. In this way, CHO provides the necessary character to fulfil its acknowledged evolutionary function: to reduce permeability while keeping high membrane fluidity [51]. This function may be extended to minimize the insertion of amphiphilic external agents, such as HePC. The CHO-containing membrane that mimics the stratum corneum (SCM) combines the low permeability given by a high sterol content with a LC character [21,22]. This feature completes the picture of this membrane of natural design as an effective barrier to the entry of external substances to the organism, corroborated by our results.

Regarding the bases of HePC as a membrane homeostasis perturbator, our results provide solid evidence that HePC can modify membrane quality. Both the rheology and the phase equilibrium of heterogeneous membranes were affected by the incorporation of HePC. The reduction of the Cs^{-1} found in all the membranes tested showed

a consistent effect of HePC in providing a more easily compressible character to the membrane, which is related to the more fluid character given by HePC previously reported in more complex model systems [18,36].

On the other hand, the presence of HePC displaced the LE-LO phase transition in LLC monolayers and LE-LC equilibrium in phospholipid monolayers, favoring the occurrence of the LE phase. In both cases, the effect evidenced a preferential partition of HePC for the LE phase, matching our surface titration experiments. This agrees with reports of a preferential partition in Lα over LO membranes for a fluorescent analogue of HePC [18] and also with the finding that HePC does not form LO domains in CHO-containing mixed bilayers [19]. An actual depletion of CHO in cell membranes has been observed after HePC treatment [52], which may be a consequence of LO domain disruption. Thus, the regulation of raft domains by HePC in the cellular environment may result in a complex interplay between a domain disrupting effect and an enhanced time of residence of CHO and HePC in the plasma membrane.

The preferential partitioning of HePC in the LE phase of DPPC monolayers was also confirmed by using a bilayer model system. HePC was able to shift the melting point of DPPC to lower temperatures characterized by a higher transition entropy. We also evidenced the equilibrium of HePC integrated into nanometer-size drug-enriched structures vs. into the DPPC enriched MLVs, matching previous fluorescence-based studies [34]. The latter micrometer-size structures showed drug saturation near 9 mol%, which is in accordance with therapeutic conditions [18].

The regulation of membrane rheology and texture evidenced here may be related to the HePC regulation of the homeostasis of CHO and choline-containing lipids, previously reported [52,53]. If we further consider that the phase state of lipid membranes is a proven factor that modulates several phospholipase activity involved in signal transduction [54–56], it is easy to picture a complex regulatory activity of HePC in lipid homeostasis.

Author contributions

The experimental work was performed by Y.M.Z.D. The project was designed and directed by M.L.F. The manuscript was written through contributions of all authors. All authors have given approval to the final version of the manuscript.

Transparency document

The Transparency document associated with this article can be found, in online version.

Acknowledgments

This work was supported by the Consejo Nacional de Investigaciones Científicas y Técnicas (CONICET) Grant number PIP 2013-2015, Agencia Nacional de Promoción Científica y Tecnológica Grant number PICT 2014-1627, and the Secretary of Science and Technology of Universidad Nacional de Córdoba Grant number 05/C578, Argentina. Y.M.Z.D. is a CONICET fellow and M.L.F. is a Career Investigator of CONICET-UNC. The authors thank Dr. Bruno Maggio and Dr. Guillermo G. Montich for useful discussions on DCS experiments. The microscopy experiments were performed in the "Centro de Microscopía Óptica y Confocal Avanzada" de Córdoba.

Appendix A. Supplementary data

Supplementary data to this article can be found online at http://dx.doi.org/10.1016/j.bbamem.2017.06.008.

References

[1] J.D.A. Pachioni, J.G. Magalhaes, E.J.C. Lima, L. de Moura Bueno, J.F. Barbosa, M. Malta de Sa, et al., Alkylphospholipids - a promising class of chemotherapeutic agents with a broad pharmacological spectrum, J. Pharm. Pharm. Sci. 16 (2013) 742–759.
[2] W.J. Van Blitterswijk, M. Verheij, Anticancer alkylphospholipids: mechanisms of action , cellular sensitivity and resistance, and clinical prospects, Curr. Pharm. Des. 14 (2008) 2061–2074, http://dx.doi.org/10.2174/138161208785294636.
[3] T.P.C. Dorlo, M. Balasegaram, J.H. Beijnen, P.J. De Vries, Miltefosine: a review of its pharmacology and therapeutic efficacy in the treatment of leishmaniasis, J. Antimicrob. Chemother. 67 (2012) 2576–2597, http://dx.doi.org/10.1093/jac/dks275.
[4] M. Dymond, G. Attard, A.D. Postle, Testing the hypothesis that amphiphilic antineoplastic lipid analogues act through reduction of membrane curvature elastic stress, J. R. Soc. Interface 5 (2008) 1371–1386, http://dx.doi.org/10.1098/rsif.2008.0041.
[5] M.P. Carrasco, J.M. Jiménez-López, J.L. Segovia, C. Marco, Hexadecylphosphocholine interferes with the intracellular transport of cholesterol in HepG2 cells, FEBS J. 275 (2008) 1675–1686, http://dx.doi.org/10.1111/j.1742-4658.2008.06322.x.
[6] A.H. Van Der Luit, M. Budde, P. Ruurs, M. Verheij, W.J. Van Blitterswijk, Alkyllysophospholipid accumulates in lipid rafts and induces apoptosis via raft-dependent endocytosis and inhibition of phosphatidylcholine synthesis, J. Biol. Chem. 277 (2002) 39541–39547, http://dx.doi.org/10.1074/jbc.M203176200.
[7] M. Saint-Pierre-Chazalet, M. Ben Brahim, L. Le Moyec, C. Bories, M. Rakotomanga, P.M. Loiseau, Membrane sterol depletion impairs miltefosine action in wild-type and miltefosine-resistant *Leishmania donovani* promastigotes, J. Antimicrob. Chemother. 64 (2009) 993–1001, http://dx.doi.org/10.1093/jac/dkp321.
[8] J.V. Busto, J. Sot, F.M. Goñi, F. Mollinedo, A. Alonso, Surface-active properties of the antitumour ether lipid 1-O-octadecyl-2-O-methyl-rac-glycero-3-phosphocholine (edelfosine), Biochim. Biophys. Acta Biomembr. 1768 (2007) 1855–1860, http://dx.doi.org/10.1016/j.bbamem.2007.04.025.
[9] S.L. Croft, K. Seifert, V. Yardley, Current scenario of drug development for leishmaniasis, Indian J. Med. Res. 123 (2006) 399–410.
[10] C.M. Rosetti, A. Mangiarotti, N. Wilke, Sizes of lipid domains: what do we know from artificial lipid membranes? What are the possible shared features with membrane rafts in cells? Biochim. Biophys. Acta Biomembr. 1859 (2017) 789–802, http://dx.doi.org/10.1016/j.bbamem.2017.01.030.
[11] I.R. Gómez-Serranillos, J. Miñones, P. Dynarowicz-Latka, J. Miñones, E. Iribarnegaray, Miltefosine-cholesterol interactions: a monolayer study, Langmuir 20 (2004) 928–933, http://dx.doi.org/10.1021/la0303254.
[12] J. Miñones, I. Rey Gómez-Serranillos, O. Conde, P. Dynarowicz-Łatka, J. Miñones Trillo, The influence of subphase temperature on miltefosine-cholesterol mixed monolayers, J. Colloid Interface Sci. 301 (2006) 258–266, http://dx.doi.org/10.1016/j.jcis.2006.04.059.
[13] M. Rakotomanga, P.M. Loiseau, M. Saint-Pierre-Chazalet, Hexadecylphosphocholine interaction with lipid monolayers, Biochim. Biophys. Acta Biomembr. 1661 (2004) 212–218, http://dx.doi.org/10.1016/j.bbamem.2004.01.010.
[14] A. Wnętrzak, K. ŁąTka, P. Dynarowicz-ŁĄtka, Interactions of alkylphosphocholines with model membranes - the langmuir monolayer study, J. Membr. Biol. 246 (2013) 453–466, http://dx.doi.org/10.1007/s00232-013-9557-4.
[15] H.M. McConnell, A. Radhakrishnan, Condensed complexes of cholesterol and phospholipids, Biochim. Biophys. Acta Biomembr. 1610 (2003) 159–173, http://dx.doi.org/10.1016/S0005-2736(03)00015-4.
[16] J. Miñones, S. Pais, J. Miñones, O. Conde, P. Dynarowicz-Łatka, Interactions between membrane sterols and phospholipids in model mammalian and fungi cellular membranes - a Langmuir monolayer study, Biophys. Chem. 140 (2009) 69–77, http://dx.doi.org/10.1016/j.bpc.2008.11.011.
[17] M. Malta de Sa, V. Sresht, C.O. Rangel-Yagui, D. Blankschtein, Understanding miltefosine-membrane interactions using molecular dynamics simulations, Langmuir 31 (2015) 4503–4512, http://dx.doi.org/10.1021/acs.langmuir.5b00178.
[18] B.M. Castro, A. Fedorov, V. Hornillos, J. Delgado, A.U. Acuña, F. Mollinedo, et al., Edelfosine and miltefosine effects on lipid raft properties: membrane biophysics in cell death by antitumor lipids, J. Phys. Chem. B 117 (2013) 7929–7940, http://dx.doi.org/10.1021/jp401407d.
[19] B. Heczková, J.P. Slotte, Effect of anti-tumor ether lipids on ordered domains in model membranes, FEBS Lett. 580 (2006) 2471–2476, http://dx.doi.org/10.1016/j.febslet.2006.03.079.
[20] M.L. Fanani, B. Maggio, Liquid-liquid domain miscibility driven by composition and domain thickness mismatch in ternary lipid monolayers, J. Phys. Chem. B 115 (2011) 41–49, http://dx.doi.org/10.1021/jp107344t.
[21] B. Školová, B. Januišš ová, J. Zbytovská, G. Gooris, J. Bouwstra, P. Slepička, et al., Ceramides in the skin lipid membranes: length matters, Langmuir 29 (2013) 15624–15633, http://dx.doi.org/10.1021/la4037474.
[22] Y. de las M Zulueta Díaz, M. Mottola, R.V. Vico, N. Wilke, M.L. Fanani, The rheological properties of lipid monolayers modulate the incorporation of L-ascorbic acid alkyl esters, Langmuir 32 (2016) 587–595, http://dx.doi.org/10.1021/acs.langmuir.5b04175.
[23] G.L. Gaines, Insoluble Monolayers at Liquid-Gas Interfaces, Interscience Publishers, New York, 1966http://dx.doi.org/10.1016/0021-9797(66)90041-5.
[24] F. Giudice, E.E. Ambroggio, M. Mottola, M.L. Fanani, The amphiphilic alkyl ester derivatives of L-ascorbic acid induce reorganization of phospholipid vesicles, Biochim. Biophys. Acta Biomembr. 1858 (2016) 2132–2139.
[25] S.C. Basu, M. Basu, Liposomes Methods and Protocols, Humana Press, Berlin, 2002http://dx.doi.org/10.1002/car.1158.
[26] S.M. Ohline, M.L. Campbell, M.T. Turnbull, S.J. Kohler, Differential scanning calorimetry of bilayer membrane phase transitions, J. Chem. Educ. (2001) 391–395.

[27] G.R. Bartlett, Colorimetric assay phosphorylated for free glyceric acids, J. Biol. Chem. 234 (1958) 469–471.
[28] N. Wilke, F. Vega Mercado, B. Maggio, Rheological properties of a two phase lipid monolayer at the air/water interface: effect of the composition of the mixture, Langmuir 26 (2010) 11050–11059, http://dx.doi.org/10.1021/la100552j.
[29] J.M. Smaby, M.M. Momsen, H.L. Brockman, R.E. Brown, Phosphatidylcholine acyl unsaturation modulates the decrease in interfacial elasticity induced by cholesterol, Biophys. J. 73 (1997) 1492–1505, http://dx.doi.org/10.1016/S0006-3495(97)78181-5.
[30] X.M. Li, J.M. Smaby, M.M. Momsen, H.L. Brockman, R.E. Brown, Sphingomyelin interfacial behavior: the impact of changing acyl chain composition, Biophys. J. 78 (2000) 1921–1931, http://dx.doi.org/10.1016/S0006-3495(00)76740-3.
[31] D. Vaknin, K. Kjaer, J. Als-Nielsen, M. Lösche, Structural properties of phosphatidylcholine in a monolayer at the air/water interface: neutron reflection study and reexamination of x-ray reflection measurements, Biophys. J. 59 (1991) 1325–1332, http://dx.doi.org/10.1016/S0006-3495(91)82347-5.
[32] L. Pedrera, A.B. Gomide, R.E. Sánchez, U. Ros, N. Wilke, F. Pazos, et al., The presence of sterols favors sticholysin i-membrane association and pore formation regardless of their ability to form laterally segregated domains, Langmuir 31 (2015) 9911–9923, http://dx.doi.org/10.1021/acs.langmuir.5b01687.
[33] K. Sabatini, J.-P.P. Mattila, P.K.J. Kinnunen, Interfacial behavior of cholesterol, ergosterol, and lanosterol in mixtures with DPPC and DMPC, Biophys. J. 95 (2008) 2340–2355, http://dx.doi.org/10.1529/biophysj.108.132076.
[34] M.B. Barioni, A.P. Ramos, M.E.D. Zaniquelli, A.U. Acuña, A.S. Ito, Miltefosine and BODIPY-labeled alkylphosphocholine with leishmanicidal activity: aggregation properties and interaction with model membranes, Biophys. Chem. 196 (2015) 92–99, http://dx.doi.org/10.1016/j.bpc.2014.10.002.
[35] D. Marsh, Lateral pressure in membranes, Biochim. Biophys. Acta Rev. Biomembr. 1286 (1996) 183–223, http://dx.doi.org/10.1016/S0304-4157(96)00009-3.
[36] L. Alonso, S.A. Mendanha, C.A. Marquezin, M. Berardi, A.S. Ito, A.U. Acuña, et al., Interaction of miltefosine with intercellular membranes of stratum corneum and biomimetic lipid vesicles, Int. J. Pharm. 434 (2012) 391–398, http://dx.doi.org/10.1016/j.ijpharm.2012.06.006.
[37] J.V. Busto, E. Del Canto-Jañez, F.M. Goñi, F. Mollinedo, A. Alonso, Combination of the anti-tumour cell ether lipid edelfosine with sterols abolishes haemolytic side effects of the drug, J. Chem. Biol. 1 (2008) 89–94, http://dx.doi.org/10.1007/s12154-008-0009-z.
[38] D.D.S. Alvares, M.L. Fanani, J. Ruggiero Neto, N. Wilke, The interfacial properties of the peptide Polybia-MP1 and its interaction with DPPC are modulated by lateral electrostatic attractions, Biochim. Biophys. Acta Biomembr. 1858 (2016) 393–402, http://dx.doi.org/10.1016/j.bbamem.2015.12.010.
[39] R.M. Weis, H.M. McConnel, Two-dimensional chiral crystals of phospholipid, Nature 310 (1984) 47–49.
[40] D. Vollhardt, Brewster angle microscopy: a preferential method for mesoscopic characterization of monolayers at the air/water interface, Curr. Opin. Colloid Interface Sci. 19 (2014) 183–197, http://dx.doi.org/10.1016/j.cocis.2014.02.001.
[41] C.W. McConlogue, T.K. Vanderlick, A close look at domain formation in DPPC monolayers, Langmuir 13 (1997) 7158–7164, http://dx.doi.org/10.1021/la970898e.
[42] P. Krüger, M. Lösche, Molecular chirality and domain shapes in lipid monolayers on aqueous surfaces, Phys. Rev. E Stat. Phys. Plasmas Fluids Relat. Interdiscip. Topics 62 (2000) 7031–7043, http://dx.doi.org/10.1103/PhysRevE.62.7031.
[43] I.R. Gomez-Serranillos, J. Miñones, P. Dynarowicz-ŁAtka, E. Iribarnegaray, M. Casas, Study of the pressure-a isotherms of miltefosine monolayers spread at the air/water interface, Phys. Chem. Chem. Phys. 6 (2004) 1580–1586.
[44] C.D. Blanchette, W.-C. Lin, C.A. Orme, T.V. Ratto, M.L. Longo, Domain nucleation rates and interfacial line tensions in supported bilayers of ternary mixtures containing galactosylceramide, Biophys. J. 94 (2008) 2691–2697, http://dx.doi.org/10.1529/biophysj.107.122572.
[45] S. Ali, S. Minchey, A. Janoff, E. Mayhew, A differential scanning calorimetry study of phosphocholines mixed with paclitaxel and its bromoacylated taxanes, Biophys. J. 78 (2000) 246–256, http://dx.doi.org/10.1016/S0006-3495(00)76588-X.
[46] D.C. Carrer, B. Maggio, Phase behavior and molecular interactions in mixtures of ceramide with dipalmitoylphosphatidylcholine, J. Lipid Res. 40 (1999) 1978–1989.
[47] T. Heimburg, Thermal Biophysics of Membranes, WILEY-VCH Verlag GmbH & Co. KGaA, Germany, 2007.
[48] M. Rakotomanga, M. Saint-Pierre-Chazalet, P.M. Loiseau, Alteration of fatty acid and sterol metabolism in miltefosine-resistant *Leishmania donovani* promastigotes and consequences for drug-membrane interactions, Antimicrob. Agents Chemother. 49 (2005) 2677–2686, http://dx.doi.org/10.1128/AAC.49.7.2677-2686.2005.
[49] P. Escobar, S. Matu, S.L. Croft, Sensitivities of *Leishmania* species to (edelfosine) and amphotericin B, Acta Trop. 81 (2002) 151–157.
[50] F.G. van der Goot, T. Harder, Raft membrane domains: from a liquid-ordered membrane phase to a site of pathogen attack, Semin. Immunol. 13 (2001) 89–97, http://dx.doi.org/10.1006/smim.2000.0300.
[51] O.G. Mouritsen, M. Bloom, The evolution of membranes, in: L. R., S. E. (Eds.), Handb. Biol. Phys, Elsevier Science, Amsterdam 1995, pp. 65–95, http://dx.doi.org/10.1139/v88-123.
[52] P. Ríos-Marco, J.M. Jiménez-López, C. Marco, J.L. Segovia, M.P. Carrasco, Antitumoral alkylphospholipids induce cholesterol efflux from the plasma membrane in HepG2 cells, J. Pharmacol. Exp. Ther. 336 (2011) 866–873, http://dx.doi.org/10.1124/jpet.110.172890.
[53] C. Marco, J.M. Jiménez-López, P. Ríos-Marco, J.L. Segovia, M.P. Carrasco, Hexadecylphosphocholine alters nonvesicular cholesterol traffic from the plasma membrane to the endoplasmic reticulum and inhibits the synthesis of sphingomyelin in HepG2 cells, Int. J. Biochem. Cell Biol. 41 (2009) 1296–1303, http://dx.doi.org/10.1016/j.biocel.2008.11.004.
[54] M. Gudmand, S. Rocha, N.S. Hatzakis, K. Peneva, K. Müllen, D. Stamou, et al., Influence of lipid heterogeneity and phase behavior on phospholipase A 2 action at the single molecule level, Biophys. J. 98 (2010) 1873–1882, http://dx.doi.org/10.1016/j.bpj.2010.01.035.
[55] M.L. Fanani, S. Hartel, B. Maggio, L. De Tullio, J. Jara, F. Olmos, et al., The action of sphingomyelinase in lipid monolayers as revealed by microscopic image analysis, Biochim. Biophys. Acta Biomembr. 1798 (2010) 1309–1323, http://dx.doi.org/10.1016/j.bbamem.2010.01.001.
[56] E.C. Ale, B. Maggio, M.L. Fanani, Ordered-disordered domain coexistence in ternary lipid monolayers activates sphingomyelinase by clearing ceramide from the active phase, Biochim. Biophys. Acta Biomembr. 1818 (2012) 2767–2776.